Promise of new imaging technologies for assessing ovarian function

Jaswant Singh[a], **Gregg P. Adams**[a], and **Roger A. Pierson**[b,*]

[a] Veterinary Biomedical Sciences, Western College of Veterinary Medicine, University of Saskatchewan, 52 Campus Drive, Saskatoon, Saskatchewan, Canada S7N 5B4

[b] Obstetrics Gynecology and Reproductive Sciences, Royal University Hospital, University of Saskatchewan, 103 Hospital Drive, Saskatoon, Saskatchewan, Canada S7N 0W8

Abstract

Advancements in imaging technologies over the last two decades have ushered a quiet revolution in research approaches to the study of ovarian structure and function. The most significant changes in our understanding of the ovary have resulted from the use of ultrasonography which has enabled sequential analyses in live animals. Computer-assisted image analysis and mathematical modeling of the dynamic changes within the ovary has permitted exciting new avenues of research with readily quantifiable endpoints. Spectral, color-flow and power Doppler imaging now facilitate physiologic interpretations of vascular dynamics over time. Similarly, magnetic resonance imaging (MRI) is emerging as a research tool in ovarian imaging. New technologies, such as three-dimensional ultrasonography and MRI, ultrasound-based biomicroscopy and synchrotron-based techniques each have the potential to enhance our real-time picture of ovarian function to the near-cellular level. Collectively, information available in ultrasonography, MRI, computer-assisted image analysis and mathematical modeling heralds a new era in our understanding of the basic processes of female and male reproduction.

Keywords

Follicle development; Folliculodynamics; Image analysis; MRI; Three-dimensional ultrasonography; Ultrasonography; Ultrasound

1. Introduction

Since the time of de Graaf, studies of follicle development involved data gathered from gross and histologic examination of excised ovaries (Jocelyn and Setchell, 1972). Even the most detailed studies of static specimens have excluded the fundamental processes of life and the mechanisms controlling them. Although knowledge gained from the study of tissue samples ex vivo has been considerable, a deeper understanding of structure–function relationships was obscured by the static nature of examination and considerable confusion about kinetics of ovarian follicle growth and development prevailed. During the 1980s a period of

*Corresponding author. Tel.: +1-306-966-4458; fax: +1-306-966-8796. pierson@erato.usask.ca (R.A. Pierson).

enlightenment in ovarian biology began with the introduction of real-time, B-mode ultrasonography. The ability to visualize changes in structure in a serial fashion, without interruption or distortion of function, has revitalized the study of ovarian biology. There has been a paradigm shift in our approaches to hypothesis testing and our understanding of folliculogenesis in domestic animals. It is now commonplace in ovarian research to include ultrasonographic imaging to monitor daily patterns of follicle growth and regression, and the ovarian response to experimental or therapeutic treatments.

Ultrasonography has heralded the way in medical imaging as a tool for ovarian research. Concurrently, continuous and rapid evolution of computer technology and medical electronics have created exciting new experimental and diagnostic capabilities in the analysis of visual data. The purpose of this manuscript is to provide an overview of imaging techniques that have been used in the study of ovarian function during the last two decades and to introduce emerging techniques that hold future promise. We begin with real-time B-mode ultrasonography and then venture through discussions of computer-assisted image analysis, three-dimensional imaging, vascular imaging, ultrasound biomicroscopy, magnetic resonance imaging (MRI), and synchrotron-based soft tissue X-ray imaging.

2. Ultrasonographic techniques in ovarian research

Gray-scale diagnostic ultrasonography is the most profound technological advance in the field of large-animal research and clinical reproduction since the introduction of transrectal palpation and radioimmunoassay of circulating hormones (Ginther, 1986). Nowhere have the effects of imaging been more evident than in the changes in our understanding of ovarian physiology. Changes in the number of peer-reviewed publications involving ovarian ultrasound imaging over the last 8 years illustrates widespread use of the technique for both research and clinical applications (Fig. 1). The technique has been used most extensively in humans and the bovine species, however, the emphasis of the ultrasound studies done in humans and animals is strikingly different. The distribution of studies in humans reflects a preoccupation with the use of ultrasonography as a tool for clinical diagnosis (i.e. detection and characterization of ovarian pathology), whereas the emphasis in animal studies is on ovarian physiology. More studies have been published on ovulation and follicular- and luteal-dynamics using the bovine model than in all other species combined. Interestingly, the use of ultrasonography has been reported frequently in both humans and animals for the study of follicular stimulation and ovulation induction, but use of the technique for oocyte retrieval has attracted more attention in animal studies even though transvaginal ultrasound-guided oocyte aspiration is the standard of practice in human assisted reproduction programs (Fig. 1).

One of the best examples of the impact of imaging on our understanding of reproductive function is that of ultrasonography and the proof of the wave-phenomenon of folliculogenesis. The wave theory of ovarian follicular development was originally proposed from observations made in the bovine species (Rajakoski, 1960). It was based on gross and histologic evaluation of ovaries obtained from cows slaughtered on known days of the estrous cycle. From his detailed studies, Rajakoski concluded that two waves of antral follicle growth occurred during the estrous cycle. Others refuted the concept of wave

phenomena and supported the notion that follicular growth is continuous and independent of the phases of the cycle (reviewed in Spicer and Echternkamp, 1986). Controversy surrounded the wave theory for nearly three decades, until the first ultrasonographic study of the bovine ovaries was reported in 1984 (Pierson and Ginther, 1984). Initial studies involved daily ultrasonography to monitor changes in follicle populations in different size categories (Pierson and Ginther, 1986, 1987a,b, 1988a). Results of these studies supported the wave theory but the population technique was not designed to monitor individually identified follicles; hence, the passage of an individual follicle from one size category to another could not be detected, and detailed characteristics of wave emergence and follicle selection were inaccessible. Hallmark studies documenting the capability of monitoring individually identified follicles soon followed (Ginther et al., 1989a,b; Knopf et al., 1989; Pierson and Ginther, 1988b; Savio et al., 1988; Sirois and Fortune, 1988). This new capability created a flurry of interest and led to a series of advancements in our understanding of folliculogenesis and the development of methods to control ovarian function in cattle and other species (Adams, 1994, 1998, 1999; Fortune, 1993; Ginther et al., 1996, 2001). One of the most important advantages arising from the use of individual identity methods or the "non-identity" method (Ginther and Bergfelt, 1992) is the ability to normalize or centralize follicular and hormonal data about a specific point of reference (e.g. ovulation, wave emergence, follicle selection). This capability led to the development of a conceptual model of the generic follicular wave that provided an explanation of temporal relationships between endocrine and structural changes (Adams and Pierson, 1995). Incorporation of the wave concept has become an inherent part of experimental design in studies of ovarian function ranging from the molecular level to the whole-animal and herd level.

The bovine model, derived from studies in mature non-pregnant cows, has since been extended to other reproductive states and other species. The first study of follicular dynamics during pregnancy and the post-partum period in any species was in cattle (Pierson and Ginther, 1986; Ginther et al., 1989c; Savio et al., 1990). The first study of follicle dynamics during the neonatal and pre-pubertal periods in any species also was in cattle in 1993 (Adams et al., 1993; Evans et al., 1994a). Studies in other species soon followed, wave patterns of follicle development were documented in each: camelids in 1990 (Adams et al., 1990), horses in 1993 (Bergfelt and Ginther, 1993), sheep and goats in 1994 (Ginther and Kot, 1994; Ravindra et al., 1994), muskoxen—the first wild species in 1997 (Hoare et al., 1997), elk in 2001 (McCorkell et al., 2001, 2002), and most recently in humans (Baerwald et al., 2002a,b, 2003). Despite the wide range of reproductive patterns represented by these different species (i.e. polyestrous, seasonally polyestrous, single and multiple ovulators, spontaneous and induced ovulators, distinct luteal and follicular phases), the fundamental wave pattern of follicle development appears to be a widely preserved biologic phenomenon.

Ultrasound imaging technology has also revolutionized the study of the corpus luteum and has led to a greater understand of the interactions between luteogenesis and folliculogenesis. For instance, it is now clear that luteal production of progesterone has a suppressive effect on the growth of the dominant follicle of a wave (Adams et al., 1992; Stock and Fortune, 1993), and the magnitude of a luteal phase (progesterone concentration and duration) has an important impact on the interwave interval, follicular health, oocyte competence and subsequent luteal gland development. It has been shown that the luteal gland does not

necessarily pass through a hemorrhagicum stage in mares (Pierson and Ginther, 1985; Ginther, 1995b). In addition, approximately 70% of bovine CL possess a fluid-filled cavity, the size of which changes during its lifespan (Kastelic et al., 1990b). In ultrasonographic studies, luteal tissue area (Kastelic et al., 1990a) and echotexture (Singh et al., 1997) was directly related to circulating and glandular concentrations of progesterone, and the presence of a fluid-filled cavity did not influence luteal function (Kastelic et al., 1990b). Ultrasonographic studies have resulted in the characterization of short luteal phases during the peri-pubertal period (Evans et al., 1994b), post-partum period (Rajamahendran and Taylor, 1990), and during seasonal recrudescence in sheep (Bartlewski et al., 1998) and elk (Adams, 1999). Luteal persistence has also been documented in relation to embryonic mortality (Kastelic and Ginther, 1989; Adams et al., 1991a), and ultrasonography has shed new light on the pathogenesis of ovarian irregularities, such as follicular and luteal cysts in cattle (Adams, 2000), hemorrhagic anovulatory follicles (HAF) in horses (Ginther, 1992) and llamas (Adams et al., 1991b), luteinized unruptured follicles (LUF) and polycystic ovarian syndrome (PCOS) in women (reviewed in Pierson and Chizen, 1994; Atiomo et al., 2000).

Ultrasound-guided techniques have provided the opportunity to collect oocytes transvaginally in mature (Pieterse et al., 1988) and prepubertal cattle (Brogliatti and Adams, 1996, Fig. 2), horses (Bracher et al., 1993; Cook et al., 1993) and in women (Wikland et al., 1983) for the purposes of in vitro embryo production. The technique has also led to novel studies involving follicular fluid sampling (Ginther et al., 1997), local or intra-follicular injections (Kot et al., 1995; Gastal et al., 1995), and gamete recovery and follicular transfer (Bergfelt et al., 1998; Hinrichs and DiGiorgio, 1991) to better understand the effects and capacity of individual follicles of a wave and their oocytes.

Ultrasonographic imaging has provided a vast improvement in our understanding of the wave pattern of folliculogenesis, but the question of why the wave pattern exists remains a mystery. We anticipate that ultrasonography and other imaging modalities will continue to stimulate scientific creativity to test hypotheses not previously conceivable.

3. Computer-assisted image analysis

Computer-assisted analysis of image attributes is a natural extension of the technologic advances in diagnostic ultrasonography. This approach offers an exciting new method of determining follicle status at a single examination. In the present section, we provide an overview of specific image analysis techniques and their applications in ovarian research and clinical diagnoses.

An ultrasonographic image is composed of thousands of picture elements, or pixels. Each pixel represents a discreet tissue reflector and can assume one of 256 shades of grey (ranging from black to white) in a 8-bit grey-scale image. The human eye can perceive "smoothness" of an image with increasing shades of grey, but can only distinguish between 18 and 20 shades of grey (Baxes, 1994). It is our contention that quantitative assessment of image data, through the use of high-resolution digital image acquisition and novel computer

algorithms will allow researchers and clinicians to assess the physiology underlying ovarian follicular growth and development (Fig. 3).

The ultrasonographic appearance or image pattern of a tissue is termed echotexture and is determined by the histologic structure of the tissue (Powis and Powis, 1984; Ginther, 1995a; Singh et al., 1997, 1998; Singh and Adams, 2000). Computer algorithms have been designed specifically for analysis of ultrasound images in an effort to overcome the inconsistencies of subjective visual evaluation, and to provide a quantitative approach to grey-scale pixel-value analysis (Synergyne 2[©], Version 1.1, WHIRL, Saskatoon, SK, Canada). These algorithms have been used extensively in studies characterizing the echotexture dynamics of ovarian structures at different phases of the follicular wave (Pierson and Adams, 1995; Singh et al., 1997, 1998; Tom et al., 1998a,b; Vassena et al., 2003).

To perform image analyses for the assessment of ovarian follicular function, each data point must be original, standardized, and easily incorporated into computer analysis software. The single most important issue in quantitative echotexture analysis is the standardization of the image during digital acquisition. Meaningful results have been obtained in vitro and in vivo in studies involving consistency in equipment (scanner and transducer) and machine settings (near-field, far-field, and overall gain) for multiple examinations of the same structures over many days (Singh et al., 1997, 1998; Tom et al., 1998a,b). It is imperative that automatic post-processing image manipulations (e.g. frame correlation) are turned off during digital acquisition. Post-acquisition image normalization of pixel values involves re-scaling the pixel values of each image to span the entire scale of 0 (black) to 255 (white), and is done to correct for inconsistencies in image digitization spanning many days (Singh et al., 1998). However, the image normalization procedure cannot correct for inconsistencies in scanner settings. It is also critical that the computer graphics files are saved in a non-destructive and uncompressed format. Some file saving and file compression algorithms (for example, JPEG and GIF formats) approximate (i.e. lose) original data. Although such compression does not affect human perception of subtle tones of grey, it renders images unsuitable for echotexture analysis. Once the computer has digitally acquired an ultrasound image, it may be manipulated like any other graphics file. In our research institute, we use a series of digital processing steps that allows us to extract numerical data (spot and line analyses), enhance visual interpretation (region analysis and time-series analysis), and automate analysis of visual data (wavelet analysis and mathematical modeling).

3.1. Spot analysis

The simplest quantitative method to analyze the pixels comprising an ultrasound image is to select one or multiple small circular areas of interest (Fig. 4A). The computer can readily determine the precise values of all of the pixels (black = 0, white = 255) within the selected spot and provide an average value (mean pixel value) and a standard deviation value (pixel heterogeneity). This simple technique is conceptually similar to spot metering techniques in photography and may be used to compare the pixel values in various portions of the image or among images at different time points. For example, portions of the follicle antrum and wall from sequential images may be evaluated to detect changes characteristic of follicular dominance, growth, atresia, impending ovulation, or luteal development and regression

(Pierson and Adams, 1995; Singh et al., 1997, 1998; Tom et al., 1998a,b; Vassena et al., 2003).

3.2. Line analysis

Similarly, a computer-generated line (thickness of 1 pixel, or more in some applications) may be drawn across a specified section of the image of the follicle to generate a graph of the grey-scale values of each pixel along the line. The graph depicts the amplitude of echoes located along the line (Fig. 4C). The two dimensions in this type of graphic display are distance (*X*-axis) and pixel value (PV) (*Y*-axis). Specific uses of this tool are to detect differences in a single follicle wall over time or among follicles. The antrum-wall interface of the follicle can be detected easily by identifying a sequential rise in grey-scale values along the line (Fig. 4C and D). Using the antrum-wall interface as a reference point, pixel values along the line can be divided into three segments, thus allowing separate analyses of the peripheral antrum, follicle wall, and stroma (Fig. 4C). Mean and peak pixel values, pixel heterogeneity, and area under the curve can be recorded separately for the three segments. In addition, pixel values along the line may be used to obtain intercept and slope values of a regression line for each of the three segments separately (Fig. 4D). To increase the precision and accuracy of analyses, numerical data may be averaged across multiple readings by placing the line-tool repeatedly across the wall of same follicle. It is important to note that care must be exercised to place the line in a region of the image free of artifacts (e.g. enhanced thorough transmission, shadowing, specular echoes, refraction, and beam-width artifacts; Kremkau, 1989; Ginther, 1995a; Heller and Jehle, 1995).

3.3. Region analysis

Region analysis of a follicle involves overlaying a pixel-by-pixel "mesh" onto a selected area (Fig. 5A) for recording pixel values at the points of intersection and generating a three-dimensional framework (Fig. 5B) or a wire-frame model. A computer generated "skin" can be placed over the mesh framework to yield a topographical surface (Fig. 5C). Shading algorithms may then be used to enhance the visual perception of surface features (Fig. 5C, surface shading, i.e. grey-scale or color assignment based on contour and direction) or echo values (height shading, i.e. grey-scale or color assignment based on "height" or brightness of pixels) of particular areas. Color application to the surfaces makes subtle differences in the surface contours easier to appreciate (Fig. 5D). In this type of display, the *X* and *Y* coordinates represent distance in two dimensions (i.e. length and width) and the *Z*-axis represents pixel value. The approach may develop into a diagnostic tool useful in clinical settings permitting instant visual assessment of ultrasonographic attributes associated with follicle health (viability or atresia).

3.4. Time series analysis

To provide information of image changes over time, a line is drawn across the follicle image, as previously described in the line analysis technique, to generate a two-dimensional graph (distance and pixel value) for the same follicle each day as it proceeds through the phases of its growth or regression. Daily graphs are then concatenated or stung together to form a composite image in a third dimension (i.e. time). An example of this type of analysis is provided which illustrates a three-dimensional graph with follicle diameter along the *X*-axis,

pixel value along the *Y*-axis and time along the *Z*-axis (Fig. 6). Shading algorithms may be applied to enhance contours, as described in region analysis. This type of analysis allows the assessment of echotextures of the follicular wall and antrum as they progress through physiologically important phases (e.g. day of dominant follicle selection, loss of dominance, atresia, day before ovulation). Time series analyses have been used in combination with other image analysis techniques to document marked differences in image characteristics associated with impending ovulation or atresia (Pierson and Adams, 1995) and detailed studies are ongoing.

3.5. Automated and semi-automated follicle recognition

A series of specialized algorithms for isolating images of follicles and follicle walls from surrounding ovarian tissues has been developed and implemented experimentally (Sarty et al., 1997; Sarty et al., 1998; Krivanek et al., 1998). This advance illustrates the potential for automated image analysis and data interpretation in ovarian biology. Study of ovarian imaging is particularly well-suited to automated analysis because of the magnitude of the interface between the follicular fluid and that of the soft tissues of the follicle wall. It is hoped that this approach may obviate the need for operator image interpretation and allow a standardized approach to interpreting ovarian and follicular physiology.

3.6. Wavelet packet texture analysis

Analysis of ultrasound images can be automated by wavelet packet texture recognition to allow clinicians to discriminate between healthy and atretic follicles. The technique involves convolve/decimate transformations (Misiti et al., 1996) of pixel values within the region of interest. In one study (Manivannan et al., 1999), the image of the follicular antrum was transformed into 85 wavelet images using three scale-levels. Wavelet classification of follicular status (healthy or atretic) appeared to be more accurate through the use of energy and standard deviation texture statistics than Euclidean minimum distance values. Although in the early stages of development, energy texture measurements based on three levels of wavelet packet transform, with or without further pure-scale transformations, hold potential as a diagnostic tool for classifying follicles.

3.7. Mathematical modeling

An interpretive mathematical approach may allow inference of hormone levels calculated from image data and thereby obviate the need for routine hormonal analyses. The procedure involves the integration of pixel-value image attributes into a comprehensive model which includes a mathematical description of the growth and regression of ovarian follicles in a competitive environment under the influence of FSH, LH, estradiol and other hormones (Sarty and Pierson, 1998, Fig. 7). In the model's simplest form, the growth of every follicle is governed by a first order, non-linear differential equation where the follicle maturity is measured by intrafollicular or circulating estradiol concentrations and image attributes (e.g. ultrasonography, MRI). Successful development of this type of modeling would provide the capability of assessing status on the basis of a single examination (diagnosis) and predicting the imminence of events (e.g. ovulation or the ovulatory potential of a follicle, optimal time for oocyte retrieval for IVF, optimal superstimulatory treatment regimen).

3.8. Physiological correlates of image attributes

In an initial characterization study, high-resolution ultrasound images of bovine follicles were obtained from ovaries excised at specific phases of follicular development (i.e. growth, early-static, late-static and regressing phases; Singh et al., 1998). The objective of the study was to determine whether quantitative changes in echotexture of dominant and subordinate follicles at different stages of development were reflective of their functional characteristics. Ultrasound images of the follicles were obtained under ideal conditions by placing the ovaries in a degassed water bath at standardized depth without interference from intervening tissues (i.e. rectal wall and adipose tissue). Follicular fluid was obtained after imaging the follicles for direct correlation. Estradiol concentrations in follicular fluid decreased from the growing to the late-static phase while progesterone content did not increase until follicles were in the final stages of regression. Detailed image analyses revealed that pixel values and heterogeneity of the antrum and wall were low in the growing, early-static and preovulatory phases of the dominant follicle. Conversely, pixel heterogeneity was characteristically high in late-static and regressing phases. The slope of the pixel value line spanning the follicle wall increased progressively from the growing to regressing phases (progressive thinning of the follicle wall); the preovulatory dominant follicle had the thickest wall and the lowest slope (Fig. 8). Pixel heterogeneity of the antrum and wall, and the slope of the follicle wall regression line were negatively correlated ($P < 0.001$) to estradiol and the estradiol:progesterone ratio in follicular fluid. It was concluded that quantitative changes in the echotexture of ultrasound images occur concurrent with changes in functional and endocrine characteristics of the bovine follicles.

When the echotexture of bovine follicles was studied by in vivo imaging, time-related changes in the walls and antra of dominant ovarian follicles were temporally associated with developmental phases of the dominant follicle as determined by serial examinations (Tom et al., 1998b). The growing phase of the dominant follicle was characterized by high pixel values of the follicle wall and decreasing antral heterogeneity. The early static phase was marked by a drop in pixel values and increased antral heterogeneity during the late static phase. The regressing phase was characterized by high mean pixel values of the follicle wall and a heterogeneous antrum (Fig. 8b). The ovulatory follicle and the dominant anovulatory follicle of Wave 1 were similar in that pixel value of the wall began to decrease 6 days after wave emergence. However, pixel values of the wall were substantially lower in images of the preovulatory follicle than those observed in the anovulatory follicle, and values for the ovulatory follicle subsequently began to increase as ovulation approached. Perhaps the observed decreases in pixel values of the dominant follicle are indicative of ovulatory potential and presage the functional transition of the follicle to a corpus luteum. This hypothesis was supported by observations reported in other studies in which the walls of late growing anovulatory and ovulatory dominant bovine follicles (Adams and Pierson, 1995) and human preovulatory follicles (Martinuk et al., 1992) exhibited darker shades of grey than those of atretic follicles.

On the premise that changes in follicle image attributes (Singh et al., 1998; Tom et al., 1998; Manivannan et al., 1999) are direct reflections of changes in follicle structure, a histomorphometric study of bovine follicles of known stages of development was performed

(Singh and Adams, 2000). The thickness of the follicle wall and granulosa layer, and vascularity of the theca interna of first wave dominant and subordinate follicles decreased progressively from growing and early-static phases to the regressing phase. In general, glandular cells, such as granulosa, theca and luteal cells appeared to be less echoic than the connective tissue stroma of the ovary. For instance, the ultrasound image of the mid-cycle bovine corpus luteum (maximal luteal cell volume at 56%) was darker than the early (angiogenic) or regressing luteal glands (luteal cells volume = 41%; Singh et al., 1997). Thus, thinning of the follicle wall during regression (Singh and Adams, 2000) resulted in a more rapid transition from the antrum (low pixel value) to the connective tissue stroma (high pixel value) leading to steeper slope values for the follicle wall (Fig. 8a). The preovulatory follicle had the thickest follicle wall, lowest cell densities in the granulosa and theca interna layers, and highest vascularity and edema in the theca interna (Singh and Adams, 2000), all of which are associated with the lowest pixel heterogeneity value and the lowest regression line slope value (Singh et al., 1998; Tom et al., 1998b). Follicle regression was characterized by detachment and release of granulosa cells from the follicle wall into the antrum (Singh and Adams, 2000). The antrum of healthy bovine follicles had very low mean pixel values while pixel heterogeneity was high in dominant follicles committed to atresia (Singh et al., 1998; Tom et al., 1998; Vassena et al., 2003) and in follicles that fail to ovulate in response to GnRH (Martinuk et al., 1992). Subordinate follicles have a brighter antrum with greater heterogeneity than their dominant counterparts (Singh et al., 1998; Vassena et al., 2003).

A relationship between image attributes and follicular function, and that between follicular status and oocyte competence have been documented (Salamone et al., 1999; Vassena, 2001). Hence, investigation of a relationship between image attributes of the ovarian follicle and the competence of the contained oocyte seemed a logical pursuit. Small to medium antral follicles from bovine ovaries obtained at the slaughterhouse have been a primary source of oocytes for in vitro embryo production in cattle. However, such follicles are in different physiologic phases (i.e. growing, static or regressing) and presumably contain oocytes with varying degrees of developmental potential. In a recent study (Vassena et al., 2003), subordinate follicles whose oocytes produced 8- to 16-cell embryos had different echotextural characteristics than follicles whose oocytes did not produce embryos. A close relationship was found between the stage of development of subordinate follicles and their ultrasound echotexture. Together with the observation that oocyte competence is associated with follicular status, thus results provided important rationale for the use of ultrasound image analysis for identifying follicles that will produce competent oocytes. Although the sensitivity of this technique is not yet sufficient for use in a diagnostic setting, the identification of statistically significant endpoints has formed the basis to improve the imaging technique. Further, the use of the remote assessment of follicular status (Pierson and Adams, 1999) brings the prospects of providing useful information in near real-time well within the grasp of practitioners or research groups who may wish to have access to the biological information, but who do not wish to invest in the computer equipment and image analysis software required to make quantitative assessments of visual data.

4. Three-dimensional ultrasonography

Conventional B-mode ultrasonography involves continuous visualization of two-dimensional "slices" of a tissue (e.g. ovary, uterus, fetus) and mental reconstruction of the tissue structure in the third dimension. This is a technically demanding procedure that has impeded exploitation of the full potential of this type of medical imaging. Advances in computing power and transducer design have made three-dimensional (3D) imaging feasible. The first generation of commercially available 3D scanners is now available from at least five ultrasound imaging equipment manufacturers. In addition, an add-on computer that can be attached to the video output of a conventional ultrasound scanner to produce a 3D image system is available from one Canadian company.

In the simplest form of three-dimensional imaging, a standard linear-array or convex-array transducer head is moved mechanically over the tissue of interest and sequential images (e.g. 30 frames/s) are captured by computer digitization. The transducer head can be moved by free-hand rotation, or mechanically by an external stepper motor assembly, or by an enclosed stepper motor within the transducer head. The 2D images are then electronically stacked together to reconstruct the tissue volume. Specific algorithms may then be applied to enhance edge detection or isolate specific image features (e.g. make the fluid around a fetus transparent so that surface contours are visible) in near real-time (i.e. within seconds of image acquisition).

A tremendous advantage of 3D imaging is that once the images are acquired and reconstructed, the image may be rotated in all different planes and evaluated without continued scanning. Further, the 3D data sets can be used to provide volumetric measurements and permit acoustic sectioning or stripping of layers of image information, revealing both internal and external features (Fig. 9). Apart from computer-related issues, many technical challenges relative to anatomy (e.g. transducer size and configuration for transrectal or transvaginal use) and subject (e.g. animal movement during image acquisition) must be resolved before 3D ultrasonography becomes a practical in animal research applications.

Three basic approaches of image acquisition for 3D reconstruction have been used (Pierson, 1999).

4.1. Angular method

A standard linear-array or convex-array transducer head is moved at a constant speed through an arc of 45°–90°, and 2D images are acquired at regular intervals. A stepper motor housing that can be adapted to fit different commercial transducers has been designed for this type of imaging (Elango et al., 1997). The complete assembly remains stationary within the rectum or vagina while the transducer head moves for 0.5 to 6 s within the assembly. The original data set takes the form of a section of a cylinder (i.e. cylindrical coordinate system); therefore, biquadratic interpolation was used to transform the data set into one representing the shape of a cube (i.e. Cartesian coordinate system). Based on this design, commercial transducers have become available as completely enclosed dedicated probes; the design is

conceptually analogous to a mechanical sector probe that contains an array of crystals rather than a single crystal.

4.2. Radial-rotation method

The radial method is suitable for use with end-fire convex-array transducers for transvaginal imaging, and involves movement of the transducer through one-half of a complete axial rotation (180° about its longitudinal axis (Kohler et al., 1997; Pierson, 1999). The reconstructed volume resembles the shape of a cone.

4.3. Matrix method

Angular and radial methods are limited by mechanical rotations of a row of crystals, but a matrix method makes use of electronic steering of ultrasound beams generated from a two dimensional matrix of crystals. Matrix probes are not yet available, but the "footprint" of such a probe will be large since the source is a sheet of piezoelectric crystals rather than a row. Matrix transducers may therefore be unsuitable for transrectal or transvaginal applications unless miniaturized versions can be developed. However, external approaches (e.g. transabdominal scanning) will be able to make use of faster acquisition times due to electronic steering of the beam.

5. Vascular imaging

The Doppler effect results from relative compression or rarefaction of sound waves from an approaching or departing source, respectively, and is the underlying reason for a change in acoustic pitch (frequency) from a moving sound source. The same principle is employed in ultrasonography to detect changes in the frequency of ultrasound waves reflected from clusters of blood cells flowing toward or away from the transducer face. Different modalities of Doppler imaging allow detection of changes in blood velocity and direction of flow over time. Other indices used to describe vascular flow characteristics, such as resistance index, pulsatility index and systolic to diastolic ratios, may be calculated. Alterations in the vasculature of the ovary occur as large follicles and corpora lutea grow and regress, and microvascular changes occur in the tissues comprising follicle walls and the luteal glands (Singh et al., 1997; Singh and Adams, 2000). Hence, in addition to study of the vascular anatomy of ovarian follicles and corpus luteum (Pierson, 1992) by color-flow Doppler imaging, important physiologic processes may also be studied by characterizing changes in vascular dynamics over time (e.g. velocity, resistance, volume). Using color flow Doppler, a pronounced "ring" of vascularity has been detected around the developing human corpus luteum (Bächström et al., 1994). Vascularity became more prominent but resistance to vascular flow decreased as the corpus luteum matured. Conversely, color mapping patterns became much less pronounced and resistance increased during luteal regression. Three variations of Doppler imaging have been used to study vascular flow: Spectral Doppler is used to display vascular flow over time in a waveform; color-flow Doppler allows superimposition of directional vascular flow information on the B-mode grey-scale imaging; and power-flow Doppler is used to superimpose low velocity vascular flow information (without directional information) on the B-mode grey-scale imaging. Color-flow and power-flow Doppler images of ovarian structures are shown, illustrating the different types of

information generated (Fig. 10). Power-flow Doppler has now been combined with color-flow Doppler to provide directional information for low velocity flow. We anticipate that as the techniques become more accessible in portable equipment, examination of blood flow patterns will become as routine and important in ovarian imaging as gray-scale ultrasonography is currently.

5.1. Spectral-flow Doppler ultrasonography

The spectral Doppler technique may involve a pulsed wave or a continuous wave. The advantage of the pulsed-wave spectral Doppler technique is that blood flow characteristics inside a specified vessel or at different regions within a cavity (e.g. heart chamber) can be measured precisely. This is made possible by the ability to place the Doppler gate (marker) at the desired anatomical location (e.g. within the lumen of vessels) using real-time ultrasonography. The ultrasound scanner then displays the spectral wave-forms over time in a different window. Quantitative data reflecting the characteristics of resistance, velocity and other characteristics may be generated. Research is just beginning on the assessment of echo-texture characteristics and vascular patterns of individual preovulatory follicles (Pierson, 2000). Although data have not yet been critically evaluated, it appears that there was a gradual decrease in impedance to blood flow in the vessels immediately surrounding the human preovulatory follicle as ovulation nears. Immediately prior to ovulation, the perifollicular vessels were easily identified; however, it is necessary to visualize the perifollicular vessels in multiple planes due to their tortuous path (Collins et al., 1991; Pierson, 2001, in press).

5.2. Color-flow Doppler ultrasonography

Color Doppler scanners display local blood flow by assigning color to mean frequency shifts. This information is then superimposed on the real-time B-mode ultrasound image. Color-flow Doppler information is directional—different colors are displayed depending on whether the blood flow is towards or away from the transducer. Changes in blood flow around preovulatory follicles and during ovulation have been demonstrated by color flow Doppler ultrasonography in women (Brannstrom et al., 1998; Pierson, 2000; Pierson, unpublished observations; Fig. 10A and C). Evaluation of ovarian blood flow during follicular stimulation treatment in women (Balakier and Stronell, 1994; Nargund et al., 1996; Oyesanya et al., 1996; Van Blerkom et al., 1997) may be interpreted to mean that that peak velocity and resistive indices decrease as the diameter of the follicles increases. A strong correlation has been observed between oocyte recovery rates and the level of follicular vascularity, and it has been proposed that perifollicular blood flow may be used to choose the optimal time for hCG administration (Oyesanya et al., 1996). Likewise, color flow ultrasonography evaluation can also be used to detect physiological or pathological changes in the corpus luteum. Low rates of luteal blood flow were observed in non-pregnant women, while corpora lutea of pregnant women had the highest rates of blood flow (Zalud and Kurjak, 1990; Glock et al., 1995). One of the problems with color-flow imaging is that artifacts resulting from random noise during ultrasonography may resemble aberrant flow in any direction, thus obscuring true flow characteristics. Other artifacts stem from intestinal motion, turbulent flow and angle-dependent measurement errors.

5.3. Power-flow Doppler ultrasonography

A new application of the Doppler technique encodes the power in the Doppler in color. This is fundamentally different from the mean frequency shift employed by color-flow Doppler imaging. Since noise has uniformly low power, when power is written in color the noise appears uniform, not random. Hence, a uniformly colored background is imaged instead of a random distribution of color, therefore, the sensitivity in measuring vascular flow is improved (Zagzebski, 1996). Power-flow Doppler information is omni-directional—all flow in tissue is shown in a single color (Fig. 10B and D). Another advantage of power Doppler imaging is that it does not alias and is relatively angle independent. The use of power Doppler imaging of the reproductive organs is in its early stages. Preliminary studies on luteal function have been performed in normal women as well as women with luteal phase defects and luteinized unruptured follicle syndrome (Kupesic and Kurjak, 1997; Kupesic et al., 1997; Zaidi et al., 1995). Follicles which fail to ovulate (luteinized unruptured follicles) showed reduced blood flow in the follicle walls after the LH surge (Zaidi et al., 1995).

6. Ultrasound biomicroscopy

The combination of B-mode ultrasonography and computer-assisted echotexture analysis has the characteristics of an ideal diagnostic tool because it would permit continuous real-time evaluation of function/dysfunction. The current generation of commercial ultrasound machines provides a lateral resolution of 0.7–1.0 mm. This level of resolution is sufficient for many clinical uses, but the full potential of image analysis can be exploited with an instrument that provides microscopic resolution (i.e. <0.2 mm). A new Canadian company has produced an ultrahigh-frequency ultrasound instrument capable of microscopic resolution (http://www.visualsonics.com). This "ultrasound biomicroscope" uses a single crystal to emit a sound wave with a frequency of 30–70 MHz and will produce an image with a resolution of 30–50 μm. To illustrate the potential of this emerging technology, a 0.7 mm ovarian follicle of an anesthetized mouse was imaged to reveal the structure of the cumulus-oocyte complex in vivo (Fig. 11). In addition, the instrument has spectral Doppler capability to measure blood flow through vessels as small as 50 μm in diameter. Major limitations of the biomicroscope are depth of penetration (approximately 10 mm at 30 MHz, 5 mm at 50 MHz), field of view (imaging width, 1 cm), and frame rate (8 frames/s). Close proximity of ovaries to the rectum and vagina in large domestic animals and humans will permit imaging with this instrument provided the instrument is used in conjunction with a conventional ultrasound machine for targeting the structures of interest. Echotexture analysis of images obtained with the ultrasound biomicroscope will, for the first time, allow the study of dynamic changes in the ovary at near histologic resolution. Serial imaging of microscopic structures over time will make accessible the study of mechanisms underlying biological events that have eluded reproductive biologists since the time of de Graaf (e.g. oocyte competence, early embryonic development and death, tubal fixation of the conceptus in humans, early luteal insufficiency, endometrial defects).

7. Magnetic resonance imaging (MRI)

7.1. Two-dimensional MRI

MRI has revolutionized the diagnosis of disease in many areas of human and veterinary medicine. MR images are less noisy and generally provide better resolution than ultrasound images (Sarty et al., 1996). Unlike speckle noise in ultrasound images (Abbott and Thurstone, 1979), the noise in MRI is not spatially correlated which makes it possible to improve signal-to-noise ratio by averaging. Magnetic resonance imaging is based upon relaxation of hydrogen protons in a large magnetic field after a radio-frequency pulse (RF) has deflected the proton spin transversely. During relaxation, T_1 recovery and T_2 decay occur simultaneously, but independently. T_1 recovery, also is known as spin-lattice relaxation, and means loss of RF pulse energy to the surrounding environment. T_2 decay, or spin–spin relaxation is the loss of energy to other protons or spins. Contrast in MR images is determined by T_1 and T_2 relaxation rates, and the proton density (PD) of tissue. The T_1 relaxation rate is the time it takes for 63% of the magnetization to recover to the longitudinal direction, or relax. The T_2 relaxation rate is the time for 63% of the transverse magnetization to be lost, or decay, while proton density is defined as the number of signal producing protons per unit volume of tissue. MR images can be weighted to preferentially reflect T_1 or T_2 relaxation as well as proton density. Two pulse sequence parameters, called T_R and T_E, govern the weighting in the image. T_1 recovery, T_2 decay and PD contribute to contrast in all MR images regardless of their weighting. An image weighted by T_1, T_2 or PD is produced by minimizing the effects of the other two processes.

Reports on the use of MRI for studying the ovaries of domestic animals are virtually non-existent because of the cost of the equipment, the relatively small size of the ovaries compared to surrounding tissues, and the narrow tube diameter that prevents placement of large animals inside the magnetic coils. However, early prototypes of magnetic coils designed for intravaginal or intrarectal use are currently being developed and may make MRI as user-friendly as ultrasonography (Sarty et al., 2001, 2002). In an effort to explore the potential advantages of MRI imaging, bovine ovaries were surgically removed at defined times of follicular wave development (Sarty et al., 1996; Hilton et al., 2000, 2001). Two dimensional T_1 and T_2 weighted images are shown (Fig. 12A and B). Antral fluid of follicles imaged prior to dominant follicle selection and during atresia had long T_1 and T_2 relaxation times. As the time of selection of the dominant follicle approached, both the T_1 and T_2 times decreased. The T_1 time decreased in dominant follicles prior to ovulation. It appears that the T_1 value is inversely related to estradiol concentrations in the follicular fluid. Thus, conventional MRI relaxometry may be useful for identifying the physiologic status of ovarian follicles. We expect that improvements in MRI speed and resolution, combined with the use of specific purpose coils, will soon allow relaxometric observations of ovarian follicles in vivo.

7.2. Three-dimensional MRI

We have used three-dimensional MR imaging coupled with maximum intensity projection display to study the topographic distribution of follicles in bovine ovaries in vitro (Sarty et al., 2000, Fig. 12C and D). Ovaries were studied using fast imaging with steady state

precession imaging sequences using maximum intensity projection which displayed three dimensional images as a cine-loop rotating in space. Presently, only the in vitro model system is functional, however, future developments making MRI fast and user-friendly make this a particularly exciting avenue of inquiry for the study of normal and pathologic ovarian function.

8. Diffraction-enhanced soft tissue X-ray imaging

The use of synchrotron light in medical imaging is an emerging field and has not been used previously to image ovarian tissue of any species. Excised bovine ovaries, and an early bovine embryo (about day 30 of gestation), were imaged using diffraction enhanced imaging (DEI) at 40 keV using a hard X-ray beamline at the National Synchrotron Light Source, Brookhaven National Laboratory, Upton, NY (Christensen et al., 2002). DEI is a new modality made possible by 2 unique characteristics of synchrotron light; i.e. the light is monochromatic (single wavelength) and polarized (single plane). In addition, synchrotron light is tremendously bright (in the order of 10^6 times brighter than the sun, at the surface of the sun) and therefore permits penetration and resolution not achievable with conventional radiography (e.g. angstroms to microns). DEI is particularly promising for soft tissue imaging because it provides exquisite contrast by using the X-ray bending properties of tissue, rather than the absorption properties. Follicles of various sizes and corpora lutea were apparent within the DE images of the ovaries; however, images of the embryo were unsatisfactory (Fig. 13). Future studies will utilize lower energies in an attempt to enhance feature contrast in ovarian and embryonic tissue, and employ computer-assisted image analysis to quantify texture differences within ovarian structures throughout the estrous cycle and pregnancy. At present, in vivo imaging of reproductive organs is not possible, but the ex vivo experiments have provided proof-of-principle that DEI of soft tissues is feasible. Future plans at the newly constructed Canadian Light Source include in vivo imaging of the ovaries in small and large animals using DEI and other modalities made possible by synchrotron light (e.g. phase contrast, K-edge subtraction).

9. Conclusion

Advancements in imaging technologies over the last two decades have ushered in a quiet revolution of research approaches to the study of ovarian structure and function. The most significant change in our understanding of the ovary have resulted from the use of ultrasonography which has enabled serial analyses in live animals. Our understanding of normal physiologic changes in the internal reproductive organs is now much clearer, as is our understanding of pathophysiologic changes. There has been rapid progression in the application of computer-assisted image analysis and mathematical modeling of the dynamic changes occuring within the ovary in vivo. In addition, new technologies, such as three-dimensional ultrasonography, two- and three-dimensional magnetic resonance imaging, ultrasound-based biomicroscopy and synchrotron-based techniques each have the potential to enhance our understanding almost to the cellular level.

Results of imaging studies over the past two decades have been promising and have far-reaching implications, well beyond the field of reproductive biology. We have developed

convincing evidence to support the underlying hypothesis that echotexture characteristics of ovarian images reflect the endocrine and physiologic status of follicles, corpora lutea, and oocytes. Data collected by various modalities provide rationale for the notion that follicles have individual characteristics; i.e. at any given stage the structural and functional status of an individual follicle may be entirely different than that of others within its cohort. In addition, early results from studies designed to correlate echotexture analysis of the follicle wall with the developmental potential of the contained oocyte have been interpreted to mean that such differences may be useful for assessing or choosing oocytes for in vitro procedures. Ultimately, through the use of imaging, we would like to be able to unravel the mysteries of ovarian function and dysfunction by detecting molecular and biochemical changes through changes in structure from the gross to cellular levels. Presently, image enhancement and echotexture analysis of images obtained by ultrasound biomicroscopy seems to be the most promising emerging technique that may allow in vivo examinations of early antral follicles and oocytes in near future. Perhaps one day we will be able to do the conceptual equivalent of Northern blot or in situ hybridization of follicular cells and gametes in vivo over time.

Acknowledgments

References

Abbott JG, Thurstone FL. Acoustic speckle: theory and experimental analysis. Ultrason Imaging. 1979; 1:303–324. [PubMed: 575829]

Adams GP. Control of ovarian follicular wave dynamics in cattle: implication for synchronization and superstimulation. Theriogenology. 1994; 41:25–30.

Adams, GP. Control of ovarian follicular wave dynamics in mature and prepubertal cattle for synchronization and superstimulation. Proceedings of the Twentieth Congress of the World Association for Buiatrics; Sydney, Australia. 1998. p. 595-605.

Adams GP. Comparative patterns of follicle development and selection in ruminants. Reproduction in domestic ruminants IV. J Reprod Fertil Suppl. 1999; 54:17–32. [PubMed: 10692842]

Adams, GP. Developments in the use of ultrasonography in buiatrics. Proceedings of the Congresso Nazionale della Societa Italiana di Buiatria; 5–7 May 2000; Stresa, Italy. 2000. p. 435-450.

Adams GP, Pierson RA. Bovine model for the study of ovarian follicular dynamics in humans. Theriogenology. 1995; 43:113–121.

Adams GP, Sumar J, Ginther OJ. Effects of lactational status and reproductive status on ovarian follicular waves in llamas (*Lama glama*). J Reprod Fertil. 1990; 90:535–545. [PubMed: 2250251]

Adams GP, Sumar J, Ginther OJ. Form and function of the corpus luteum in llamas. Anim Reprod Sci. 1991a; 24:127–138.

Adams GP, Sumar J, Ginther OJ. Hemorrhagic ovarian follicles in llamas. Theriogenology. 1991b; 35:557–568. [PubMed: 16726925]

Adams GP, Matteri RL, Ginther OJ. Effect of progesterone on ovarian follicles, emergence of follicular waves and circulating follicle-stimulating hormone in heifers. J Reprod Fertil. 1992; 95:627–640.

Adams GP, Evans ACO, Rawlings NC. Follicular waves and circulating gonadotropins in 8-month old prepubertal heifers. J Reprod Fertil. 1993; 100:27–33.

Atiomo WU, Pearson S, Shaw S, Prentice A, Dubbins P. Ultrasound criteria in the diagnosis of polycystic ovary syndrome (PCOS). Ultrasound Med Biol. 2000; 26:977–980. [PubMed: 10996697]

Bächström, T., Nakata, M., Pierson, RA. Ultrasonography of normal and abnormal luteogenesis. In: Jaffe, R.Pierson, RA., Abramowicz, JS., editors. Imaging in Infertility and Reproductive Endocrinology. Lippincott; Philadelphia: 1994. p. 143-154.

Baerwald, AR., Adams, GP., Pierson, RA. A new model for the menstrual cycle in women. Proceedings of the 11th World Congress on Human Reproduction; Montreal, Que. 2002a. (abstract #29)

Baerwald AR, Adams GP, Pierson RA. Folliculogenesis revisited: characteristics of ovarian follicular waves during the menstrual cycle. Fertil Steril. 2002b; 78(3 Suppl 1):S67.

Baerwald AR, Adams GP, Pierson RA. A new model for folliculogenesis during the menstrual cycle in women. Fertil Steril. 2003 in press.

Balakier H, Stronell RD. Color doppler assessment of folliculogenesis in vitro fertilization patients. Fertil Steril. 1994; 62:1211–1216. [PubMed: 7957986]

Bartlewski PM, Beard AP, Cook SJ, Rawlings NC. Ovarian follicular dynamics during anoestrus in ewes. J Reprod Fertil. 1998; 113:275–285. [PubMed: 9861168]

Baxes, GA. Digital Image Processing: Principles and Applications. Wiley; New York: 1994. Fundamentals of digital image processing; p. 13-36.

Bergfelt DR, Ginther OJ. Relationship between FSH surges and follicular waves during the estrous cycle in mares. Theriogenology. 1993; 39:781–796. [PubMed: 16727253]

Bergfelt DR, Brogliatti GM, Adams GP. Gamete recovery and follicular transfer (GRAFT) using transvaginal ultrasonography in cattle. Theriogenology. 1998; 50:15–25. [PubMed: 10734470]

Bracher V, Parlevliet J, Fazelli AR, Pieterse MC, Vos PL, Dielmeman SJ, Taverne MA, Colenbrander B. Repeated transvaginal ultrasound-guided follicle aspiration in the mare. Equine Vet J Suppl. 1993; 15:75–78.

Brannstrom M, Zackrisson U, Hagstrom HG, Josefsson B, Hellberg P, Granberg S, Collins WP, Bourne T. Preovulatory changes of blood flow in different regions of the human follicle. Fertil Steril. 1998; 69:435–442. [PubMed: 9531873]

Brogliatti GM, Adams GP. Ultrasound-guided transvaginal oocyte collection in prepubertal calves. Theriogenology. 1996; 45:1163–1176. [PubMed: 16727873]

Christensen, CR., Singh, J., Adams, GP. The use of diffraction enhanced imaging for bovine soft tissue. Proceedings of the Fifth Annual Users' Meeting and Workshops of the Canadian Light Source; 15–16 November 2002; Saskatoon: University of Saskatchewan; 2002. p. 26(abstract #35)

Collins W, Jurkovic D, Bourne T, Kurjak A, Campbell S. Ovarian morphology, endocrine function and intra-follicular blood flow during the peri-ovulatory period. Hum Reprod. 1991; 6:319–324. [PubMed: 1955534]

Cook NL, Squires EL, Ray BS, Jasko DJ. Transvaginal ultrasound-guided follicular aspiration of equine oocytes. Equine Vet J Suppl. 1993; 15:71–74.

Elango, A., Gander, RE., Adams, GP. Design and development of a three-dimensional ultrasound transducer for veterinary applications. Proceedings of the Annual Conference of the Canadian Medical and Biological Engineering Society; Toronto, ON, Canada. 1997. p. 74-75.

Evans ACO, Adams GP, Rawlings NC. Follicular and hormonal development in prepubertal heifers from 2 to 36 weeks of age. J Reprod Fertil. 1994a; 102:463–470. [PubMed: 7861402]

Evans ACO, Adams GP, Rawlings NC. Endocrine and ovarian follicular changes leading up to the first ovulation in prepubertal heifers. J Reprod Fertil. 1994b; 100:187–194. [PubMed: 8182588]

Fortune JE. Follicular dynamics during the bovine estrous cycle: a limiting factor in improvement of fertility? Anim Reprod Sci. 1993; 33:111–125.

Gastal EL, Kot K, Ginther OJ. Ultrasound-guided intrafollicular treatment in mares. Theriogenology. 1995; 44:1027–1037. [PubMed: 16727797]

Ginther, OJ. Ultrasonic imaging and reproductive events in the mare. Equiservices Publishing; Cross Plains, WI: 1986.

Ginther, OJ. Reproductive Biology of the Mare. 2. Equiservices Publishing; Cross Plains, WI: 1992. p. 224

Ginther, OJ. Ultrasonic Imaging and Animal Reproduction: Fundamentals Book 1. Equiservices Publishing; Cross Plains, WI: 1995a. p. 7-82.p. 35-40.p. 147-155.

Ginther, OJ. Ultrasonic Imaging and Animal Reproduction: Horses. Equiservices Publishing; Cross Plains, WI: 1995b. p. 35-40.p. 77-83.

Ginther OJ, Bergfelt DR. Ultrasonic characterization of follicular waves in mares without maintaining identity of individual follicles. J Equine Vet Sci. 1992; 12:349–354.

Ginther OJ, Kot K. Follicular dynamics during the ovulatory season in goats. Theriogenology. 1994; 42:987–1001. [PubMed: 16727603]

Ginther OJ, Beg MA, Bergfelt DR, Donadeu FX, Kot K. Follicle selection in monovular species. Biol Reprod. 2001; 65:638–647. [PubMed: 11514323]

Ginther OJ, Kastelic JP, Knopf L. Composition and characteristics of follicular waves during the bovine estrous cycle. Anim Reprod Sci. 1989a; 20:187–200.

Ginther OJ, Knopf L, Kastelic JP. Temporal associations among ovarian events in cattle during oestrous cycles with 2 and 3 follicular waves. J Reprod Fertil. 1989b; 87:223–230. [PubMed: 2621698]

Ginther OJ, Knopf L, Kastelic JP. Ovarian follicular dynamics in heifers during early pregnancy. Biol Reprod. 1989c; 41:247–254. [PubMed: 2679900]

Ginther OJ, Wiltbank MC, Fricke PM, Gibbons J, Kot K. Selection of the dominant follicle in cattle. Biol Reprod. 1996; 55:1187–1194. [PubMed: 8949873]

Ginther OJ, Kot K, Kulick LJ, Wiltbank MC. Sampling follicular fluid without altering follicular status in cattle: oestradiol concentrations early in a follicular wave. J Reprod Fertil. 1997; 109:181–186. [PubMed: 9155725]

Glock JL, Blackman JA, Dadger GJ, Brumstead JR. Prognostic significance of morphologic changes of the corpus luteum by transvaginal ultrasound in early pregnancy monitoring. Obstet Gynecol. 1995; 85:37–41. [PubMed: 7800321]

Heller, M., Jehle, D. Ultrasound in Emergency Medicine. Saunders; Philadelphia: 1995. p. 1-40.

Hilton JE, Sarty GE, Adams GP, Pierson RA. Magnetic resonance image attributes of the bovine ovarian follicle antrum during development and regression. J Reprod Fertil. 2000; 120:311–323. [PubMed: 11058447]

Jocelyn HD, Setchell BP. Regnier de Graaf on the human reproductive organs. An annotated translation of Tractatus de Virorum Organis Generationi Inservientibus (1668) and De Mulierub Organis Generationi Inservientibus Tractatus Novus (1962). J Reprod Fertil Suppl. 1972; 17:1–222. [PubMed: 4567037]

Hinrichs K, DiGiorgio LM. Embryonic development after intrafollicular transfer of horse oocyte. J Reprod Fertil Suppl. 1991; 44:369–374. [PubMed: 1795280]

Hoare EK, Parker SE, Flood PF, Adams GP. Ultrasonic imaging of reproductive events in muskoxen. Rangifer. 1997; 17:119–123.

Kastelic JP, Ginther OJ. Fate of conceptus and corpus luteum after induced embryonic loss in heifers. J Am Vet Med Assoc. 1989; 194:922–928. [PubMed: 2649472]

Kastelic JP, Bergfelt DR, Ginther OJ. Relationship between ultrasonic assessment of the corpus luteum and plasma progesterone concentration in heifers. Theriogenology. 1990a; 33:1269–1278.

Kastelic JP, Pierson RA, Ginther OJ. Ultrasonic morphology of corpora lutea and central cavities during the estrous cycle and early pregnancy in heifers. Theriogenology. 1990b; 34:487–498. [PubMed: 16726855]

Knopf L, Kastelic JP, Schallenberger E, Ginther OJ. Ovarian follicular dynamics in heifers: test of two-wave hypothesis by ultrasonically monitoring individual follicles. Dom Anim Endocr. 1989; 6:111–119.

Kohler, J., Gander, RE., Pierson, RA. Development of intravaginal three-dimensional ultrasonography. Proceedings of the Conference of the Canadian Medical and Biological Engineering Society; 1997. p. 134-135.

Kot K, Gibbons JR, Ginther OJ. A technique for intrafollicular injection in cattle: effects of hCG. Theriogenology. 1995; 44:41–50.

Kremkau, FW. Diagnostic Ultrasound: Principles, Instruments, and Exercises. Saunders; Philadelphia: 1989. p. 1-50.p. 147-176.p. 219-231.

Krivanek, A., Liang, W., Sarty, G., Pierson, RA., Sonka, M. Automated follicle analysis in ovarian ultrasound medical imaging 1998: image processing. Proceedings of the International Society for Optical Engineering (SPIE); 1998. p. 3338p. 588-596.

Kupesic S, Kurjak A, Vujisic S, Petrovic Z. Luteal phase defect: comparison between Doppler velocimetry, histological and hormonal markers. Ultrasound Obstet Gynecol. 1997; 9:105–112. [PubMed: 9132252]

Kupesic S, Kurjak A. The assessment of normal and abnormal luteal function by transvaginal color Doppler sonography. Eur J Obstet Gynecol Reprod Biol. 1997; 72:83–87. [PubMed: 9076427]

Manivannan U, Sarty GE, Sirounis H, Singh J, Adams GP, Pierson RP. Physiologic classification of bovine ovarian follicles with wavelet packet texture analysis. SPIE. 1999; 3661:1238–1245.

Martinuk SD, Chizen DR, Pierson RA. Ultrasonographic morphology of the human preovulatory follicle wall prior to ovulation. Clin Anat. 1992; 5:1–14.

McCorkell, RB., MacDougall, L., Adams, GP. Transrectal ultrasonography in female Wapiti (*Cervus elaphus*): a feasibility study. In: Renecker, LA., Renecker, TA., editors. Game Conservation and Sustainability: Biodiversity, Management, Ecotourism, Traditional Medicine and Health. Stratford; ON, Canada: 2001. p. 282-290.

McCorkell RB, MacDougall L, Adams GP. Ovarian follicle development in Wapiti (*Cervus elaphus*) during the anestrous season. Theriogenology. 2002 in press.

Misiti, M., Misiti, Y., Oppenheim, G., Poggi, JM. Wavelet Toolbox Users's Guide. The Math Works Inc; Natick, Mass: 1996.

Nargund G, Bourne T, Doyle P, Parsons J, Cheng W, Campbell S, Collins W. Associations between ultrasound indices of follicular blood flow, oocyte recovery and preimplantation embryo quality. Hum Reprod. 1996; 11:109–113.

Oyesanya OA, Parsons JH, Collins WP, Campbell S. Prediction of oocyte recovery rate by transvaginal ultrasonography and color Doppler imaging before human chorionic gonadotropin administration in vitro fertilization cycles. Fertil Steril. 1996; 65:806–809. [PubMed: 8654643]

Pierson, RA. From ovulation to implantation. In: Jaffe, R., Warsof, S., editors. Color Doppler Imaging in Obstetrics and Gyanecology. McGraw-Hill; New York: 1992. p. 35-60.

Pierson, RA. Three-dimensional ultrasonography of the embryo and fetus. In: Jaffe, R., Bui, T-H., editors. Fetal and Neonatal Ultrasonography. Parthenon Publishing Group; New York: 1999. p. 317-326.

Pierson, RA. Imaging technology in assisted reproduction. In: Wolf, D., Zelinski-Wooten, M., editors. Assisted Reproduction and Nuclear Transfer in Mammals. Humana Press; Totowa, NJ: 2000. p. 95-122.

Pierson RA, Adams GP. Computer-assisted image analysis, diagnostic ultrasonography and ovulation induction: strange bedfellows. Theriogenology. 1995; 43:105–112.

Pierson RA, Adams GP. Remote assessment of ovarian response and follicular status using visual data analysis of ultrasonographic images. Theriogenology. 1999; 51:47–57. [PubMed: 10729061]

Pierson, RA., Chizen, DR. Transvaginal ultrasonographic assessment of normal and aberrant ovulation. In: Jaffe, R.Pierson, RA., Abramowicz, JS., editors. Imaging in Infertility and Reproductive Endocrinology. Lippincott; Philadelphia: 1994. p. 129-142.

Pierson RA, Ginther OJ. Ultrasonography of the bovine ovary. Theriogenology. 1984; 21:495–504. [PubMed: 16725899]

Pierson RA, Ginther OJ. Ultrasonic evaluation of the corpus luteum of the mare. Theriogenology. 1985; 23:795–806. [PubMed: 16726050]

Pierson RA, Ginther OJ. Ovarian follicular populations during early pregnancy in heifers. Theriogenology. 1986; 26:649–659. [PubMed: 16726232]

Pierson RA, Ginther OJ. Follicular populations during the estrous cycle in heifers: Part I. Influence of day. Anim Reprod Sci. 1987a; 124:165–176.

Pierson RA, Ginther OJ. Follicular populations during the estrous cycle in heifers. Part II Influence of right and left sides and intraovarian effect of the corpus luteum. Anim Reprod Sci. 1987b; 14:177–186.

Pierson RA, Ginther OJ. Follicular populations during the estrous cycle in heifers. Part III Time of selection of ovulatory follicle. Anim Reprod Sci. 1988a; 16:81–95.

Pierson RA, Ginther OJ. Ultrasonic imaging of the ovaries and uterus in cattle. Theriogenology. 1988b; 29:21–37.

Pieterse MC, Kappen RA, Kruip AM, Taverne MAM. Aspiration of bovine oocyte during transvaginal ultrasound scanning of the ovaries. Theriogenology. 1988; 30:751–762. [PubMed: 16726517]

Powis, R., Powis, W. A Thinker's Guide to Ultrasonic Imaging. Urban and Schwartzenberg Inc; Baltimore, MD: 1984.

Rajakoski E. The ovarian follicular system in sexually mature heifers with special reference to seasonal, cyclical, and left-right variations. Acta Endocr Copenh Suppl. 1960; 52:7–68.

Rajamahendran R, Taylor C. Characterization of ovarian activity in postpartum dairy cows using ultrasound imaging and progesterone profiles. Anim Reprod Sci. 1990; 22:171–180.

Ravindra JP, Rawlings NC, Evans ACO, Adams GP. Ultrasonographic study of ovarian follicular dynamics in ewes during the oestrous cycle. J Reprod Fertil. 1994; 101:501–509. [PubMed: 7932387]

Salamone DF, Adams GP, Mapletoft RJ. Changes in the cumulus–oocyte complex of subordinate follicles relative to follicular wave status in cattle. Theriogenology. 1999; 52:549–561. [PubMed: 10734355]

Sarty GE, Pierson RA. Analysis of ovarian follicular response to superstimulation in a three-dimensional parametric space. Fertil Steril. 1998; 70 (Suppl 3):S183.

Sarty GE, Adams GP, Pierson RA. Three-dimensional magnetic resonance imaging for the study of ovarian function in bovine in vitro model. J Reprod Fertil. 2000; 119:69–75. [PubMed: 10864815]

Sarty GE, Baerwald AR, Loewy J, Pierson RA. External versus internal magnetic resonance imaging methods for the study of ovarian structure and function. MAG*MA. 2002 in press.

Sarty, GE., Hess, AR., Baerwald, Loewy, J., Pierson, RA. External versus intravaginal mri for ovarian imaging. Proceedings of the 47th Annual Meeting of the Canadian Fertility and Andrology Society; Whistler, BC. 2001. (Abstract 58a)

Sarty GE, Kendall EJ, Pierson RA. Magnetic resonance imaging of bovine ovaries in vitro. Mag Res Mat Physics Biol Med (MAG*MA). 1996; 4:205–211.

Sarty, GE., Liang, W., Sonka, M., Pierson, RA. The Development of a Semi-Automated Segmentation of Ovarian Follicular Images Using a Knowledge-Based Algorithm. Medical Imaging 1997: Image Processing; Proceedings of the International Society for Optical Engineering (SPIE); 1997. p. 822-829.

Sarty GE, Liang W, Sonka M, Pierson RA. Semi-automated segmentation of ovarian follicular ultrasound images using a knowledge-based algorithm. J Ultrasound Med Biol. 1998; 24:27–42.

Savio JD, Boland MP, Hynes N, Roche JF. Resumption of follicular activity in the early postpartum period of dairy cows. J Reprod Fertil. 1990; 88:569–579. [PubMed: 2182844]

Savio JD, Keenan L, Boland MP, Roche JF. Pattern of growth of dominant follicles during the estrous cycle of heifers. J Reprod Fertil. 1988; 83:663–671. [PubMed: 3045306]

Singh J, Adams GP. Histomorphometry of dominant and subordinate bovine ovarian follicles. Anat Rec. 2000; 258:58–70. [PubMed: 10603449]

Singh J, Pierson RA, Adams GP. Ultrasound image attributes of the bovine corpus luteum: structural and functional correlates. J Reprod Fertil. 1997; 109:35–44. [PubMed: 9068411]

Singh J, Pierson RA, Adams GP. Ultrasound image attributes of bovine ovarian follicles: endocrine and functional correlates. J Reprod Fertil. 1998; 112:19–29. [PubMed: 9538326]

Sirois J, Fortune JE. Ovarian follicular dynamics during the estrous cycle in heifers monitored by real-time ultrasonography. Biol Reprod. 1988; 39:308–317. [PubMed: 3052602]

Spicer LJ, Echternkamp SE. Ovarian follicular growth, function and turnover in cattle: a review. J Anim Sci. 1986; 62:428–451. [PubMed: 3007421]

Stock AE, Fortune JE. Ovarian follicular dominance in cattle: relationship between prolonged growth of the ovulatory follicle and endocrine parameters. Endocrinology. 1993; 132:1108–1114. [PubMed: 8440173]

Tom JW, Pierson RA, Adams GP. Quantitative echotexture analysis of bovine corpora lutea. Theriogenology. 1998a; 49:1345–1352. [PubMed: 10732071]

Tom JW, Pierson RA, Adams GP. Quantitative echotexture analysis of bovine ovarian follicles. Theriogenology. 1998b; 50:339–346. [PubMed: 10732129]

Van Blerkom J, Antczak M, Schrader R. The developmental potential of the human oocyte is related to the dissolved oxygen content of follicular fluid: association with vascular endothelial growth factor levels and perifollicular blood flow characteristics. Hum Reprod. 1997; 12:1047–1055. [PubMed: 9194664]

Vassena, R. MSc Thesis. University of Saskatchewan; Saskatoon, Canada: 2001. Bovine Oocyte Competence.

Vassena R, Adams GP, Mapletoft RJ, Pierson RA, Singh J. Ultrasound image characteristics of ovarian follicles in relation to oocyte competence and follicular status in cattle. Anim Reprod Sci. 2003; 76:25–41. [PubMed: 12559718]

Wikland M, Nilsson L, Hansson R, Hamberger L, Janson PO. Collection of human oocytes by the use of sonography. Fertility Sterility. 1983; 38:603–608.

Zagzebski, J. Essentials of Ultrasound Physics. Mosby-Year Book, Inc; St. Louis, MO: 1996. Doppler instrumentation; p. 87-108.

Zaidi J, Jurkovic D, Campbell S, Collins W, McGregor A, Tan SL. Luteinized unruptured follicle: morphology, endocrine function and blood flow changes during the menstrual cycle. Hum Reprod. 1995; 10:44–49. [PubMed: 7745069]

Zalud I, Kurjak A. The assessment of luteal blood flow in pregnant and non-pregnant women by transvaginal color Doppler. J Perinat Med. 1990; 18:215–221. [PubMed: 2200864]
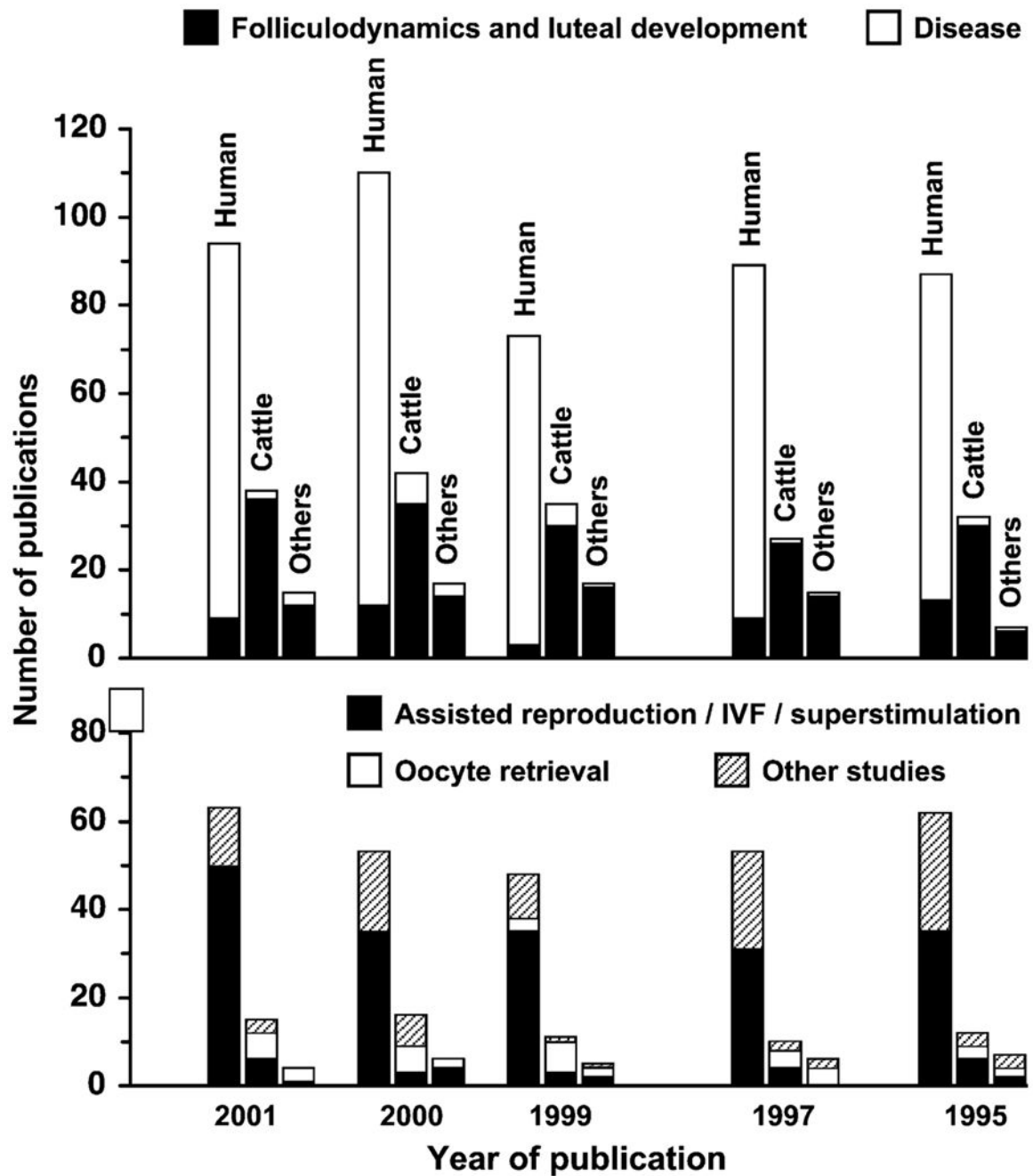
Fig. 1.
Demographics of publications on ultrasound-based ovarian research in human, cattle, horse and other domestic species over the last 8 years. Data were obtained by searching for keywords—(ultrasound or ultrasonography) and (ovary or follicle or corpus luteum) in Agricola, Medline and CAB databases for human, cattle and other species (sheep, goat, mare, camlids, pig). Based on the title and year of publication, number of publications for each species were categorized into (i) folliculodynamics and luteal development, (ii) disease, (iii) assisted reproduction/IVF/superstimulation and (iv) other studies.
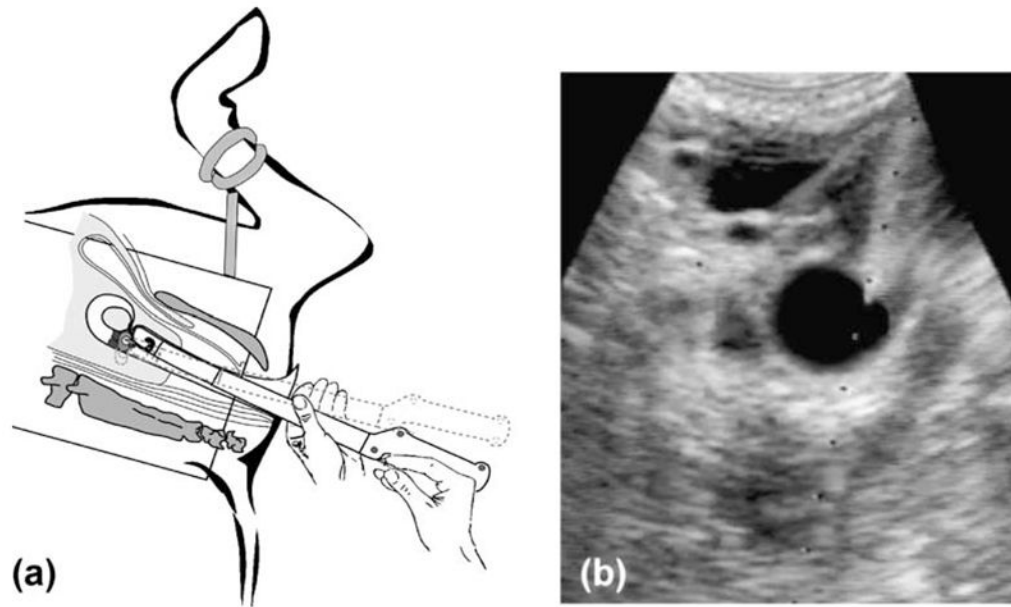
Fig. 2.
Ultrasound-guided follicle aspiration technique for calves. (a) Demonstrates the topography of the genital organs and position of the transducer for transvaginal ultrasonography and oocyte aspiration in 6 week-old calves in dorsal recumbency. (b) Ultrasound image of an ovarian follicle during the aspiration procedure. The image of the needle entering the anechoic follicle is clearly observed (modified with permission from Brogliatti and Adams, 1996).
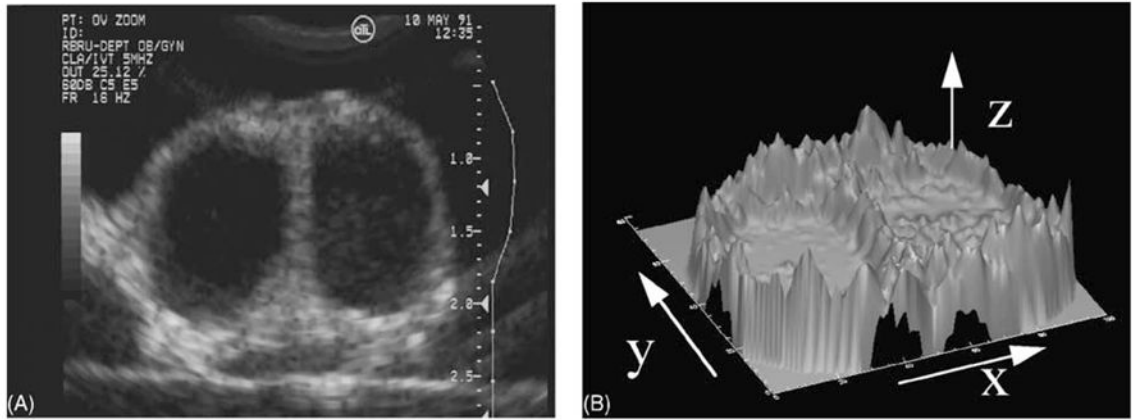
Fig. 3.
(A) To illustrate the sensitivity of computer-assisted data analysis, an excised bovine ovary containing a preovulatory (left) and a regressing (right) follicle was scanned in a degassed water bath using a high resolution ultrasound instrument. The two large follicles imaged appear visually indistinguishable (B) Clear differences in the follicle walls and antra can be detected by computer-assisted analyses. In a three-dimensional representation of the brightness of the pixels comprising the ultrasound image, the echotexture of the antrum appears more heterogeneous and the pixels of the follicular wall are brighter and drop off more sharply in the follicle on the right. Image attributes were consistent with the notion that the follicle on the left was the dominant follicle of a new wave, while the follicle on the right was the dominant follicle of a previous wave (modified with permission from Adams and Pierson, 1995).
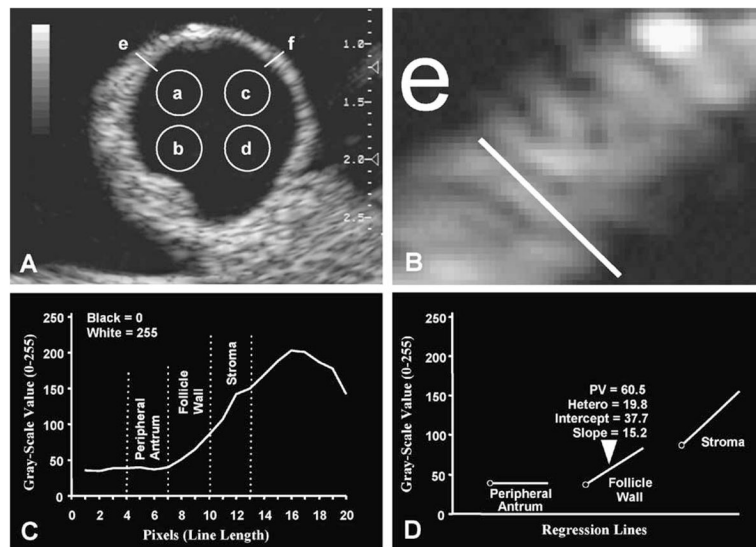
Fig. 4.
(A, B) Computer-assisted analysis of ultrasound image of an ovarian follicle. Portion of the follicle wall from part A is enlarged in part B to display the picture-elements (pixels) forming the ultrasound image. Spot-analysis of the antrum is performed to measure the pixel value (black = 0, white = 255) and pixel heterogeneity by placing the measuring circle at four different locations (a, b, c, d) over the follicle antrum to cover approximately 20% of the area in each quadrant. (C) Line-analysis of the peripheral antrum, follicle wall and stroma was performed by placing a computer-generated line on the ultrasonographic image at 10 and 2 o'clock positions (e, f on part A, e on part B) and plotting the gray-scale values of pixels along the line. The pixel value graph was divided into three segments (peripheral antrum, follicle wall, stroma). The antrum-wall interface was used as a reference point. (D) Pixel value (PV), pixel heterogeneity (Hetero), and the intercept and slope of the regression line of each segment is recorded separately (modified with permission from Singh et al., 1998).
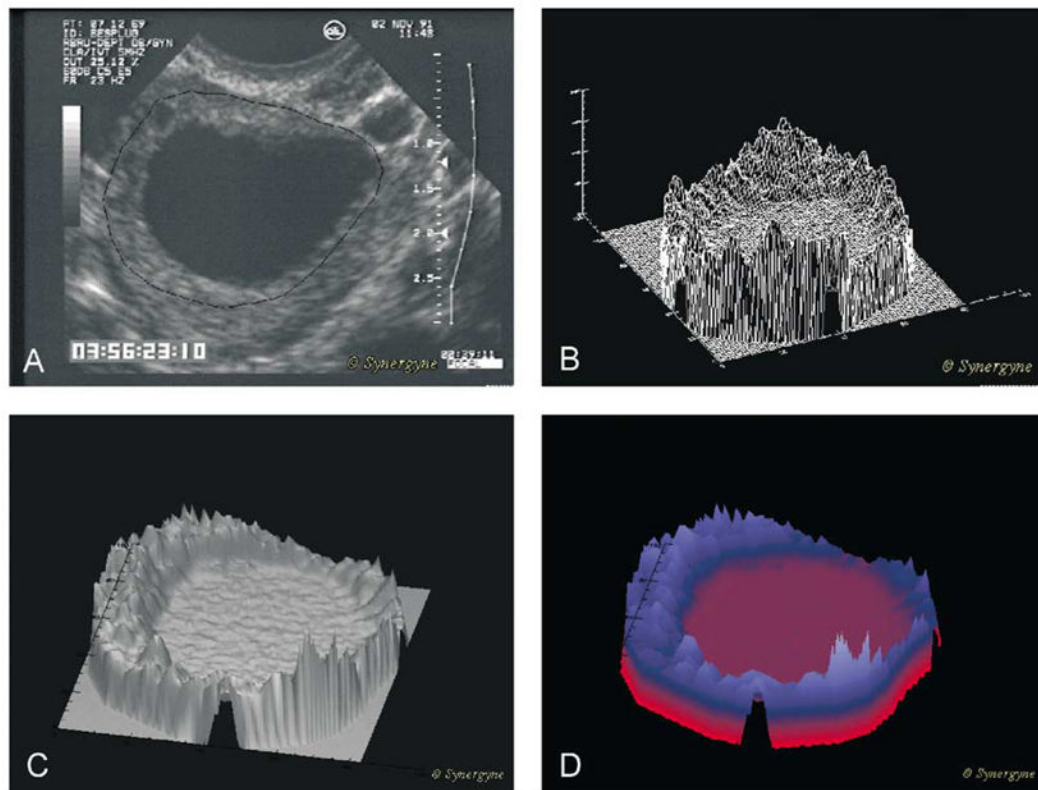
Fig. 5.
Regional analysis of a single human preovulatory follicle. (A) Image of the follicle with follicle wall identified (black line). (B) Wire-frame model of the pixel by pixel mesh created from the image of the follicle. (C) Computer generated "skin" stretched over the wire-frame model. (D) Height shaded color algorithm added to the image to enhance visual appreciation and allow comparison of different zones with images of different follicles or images of the same follicle on different days.
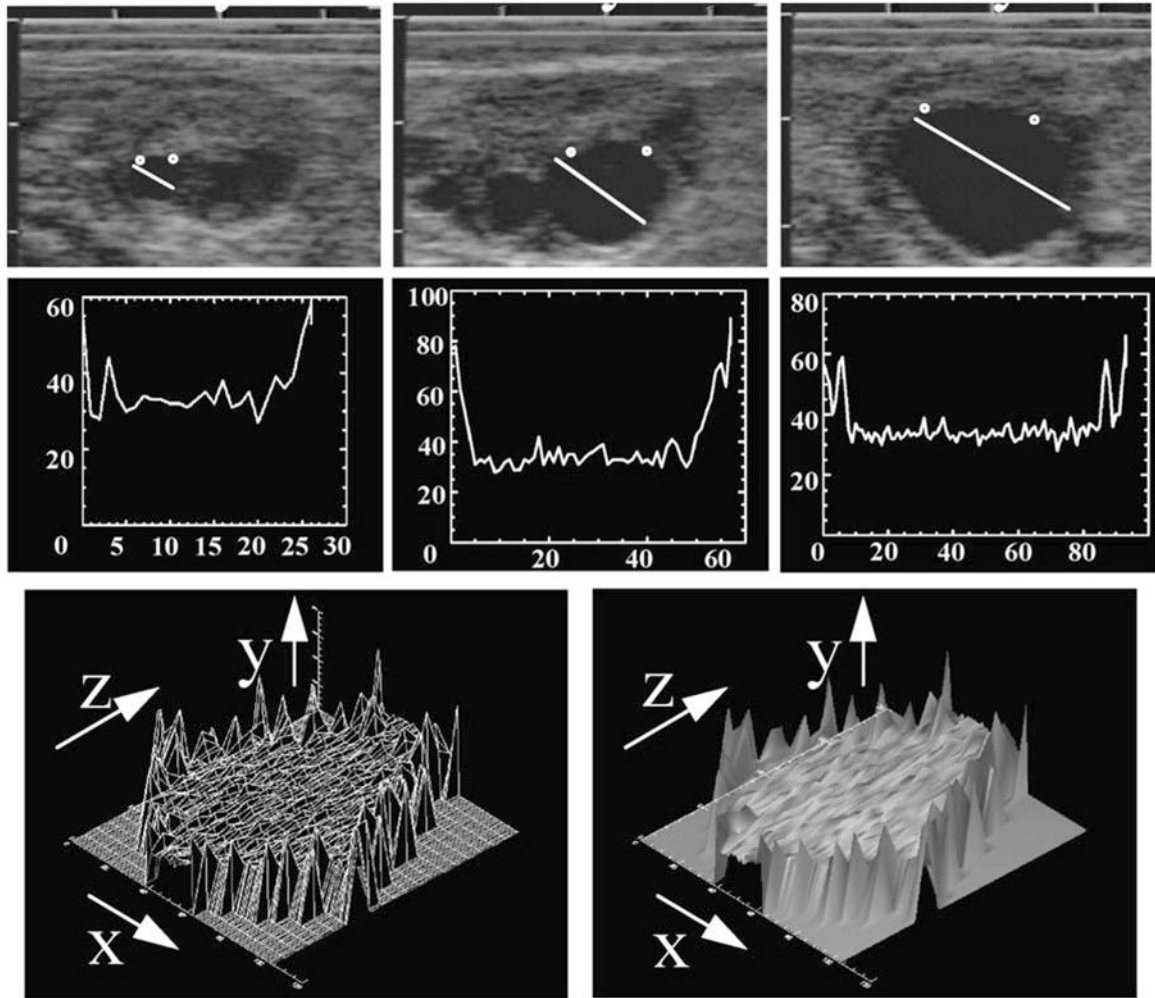
Fig. 6.
Time-series analysis of a dominant anovulatory follicle. Individual follicles are identified (top three panels) on a daily basis and a graphic line representing their numerical values created (second three panels). The numerical values are concatenated and a wire-mesh framework created (lower left panel). The X dimension represents the diameter of the follicle including the follicle wall, the Y dimension represents the numerical pixel value, and the Z dimension represents the days of the cycle on which the follicle was uniquely identified. A surface rendering (skin) is placed over the framework to yield a conceptualization of the physiologic status of the follicle (lower right panel) from the time that the follicle was first identified, completes its growth phase, enters and passes through a static phase, and then regressed until it could no longer be identified. Addition of color shading algorithms adds to greatly enhanced visual perception.
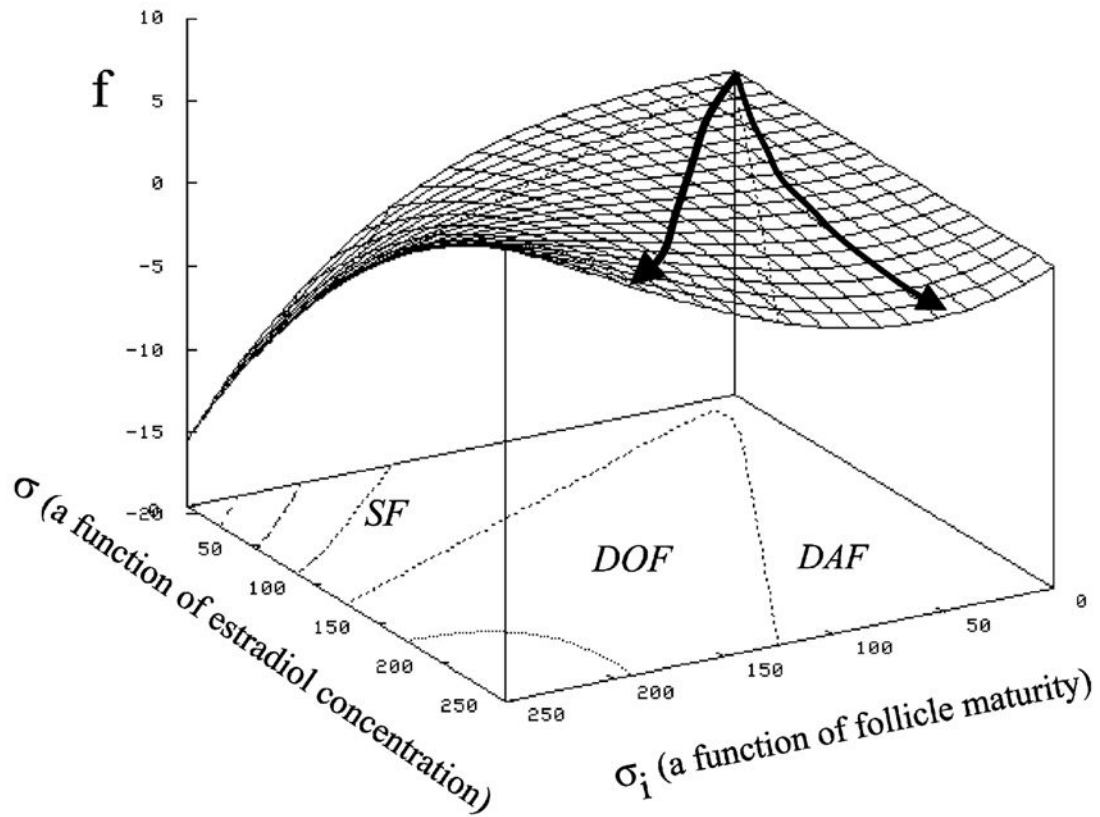
Fig. 7.
Three dimensional parametric space model of ovarian follicular development. Maturity, m, of the follicles was equated to diameter. The rate of growth of the follicle z was determined by using central finite differences from the ultrasonographic time series data. The maturation rate (pg E_2 per hour calculated based on daily blood samples, ξ reflects circulating E_2 and ξ_i reflects maturity. SF represents the spatial area of subordinant follicles, DOF that occupied by dominant ovulatory follicles and DAF the area associated with dominant anovulatory follicles. The data were then plotted in the three dimensional (z, m, E_2) parametric space and interpolated to yield a mathematical maturation surface. We are interested in modifying this model to include image attributes, like echotexture and follicle size, and the effects of pathology and pharmacologic intervention which will yield interpretive models. On the surface framework, the line to the left illustrates the developmental history of a dominant ovulatory follicle while the line to the right illustrates the history of an dominant anovulatory follicle (modified from Sarty and Pierson, 1998).
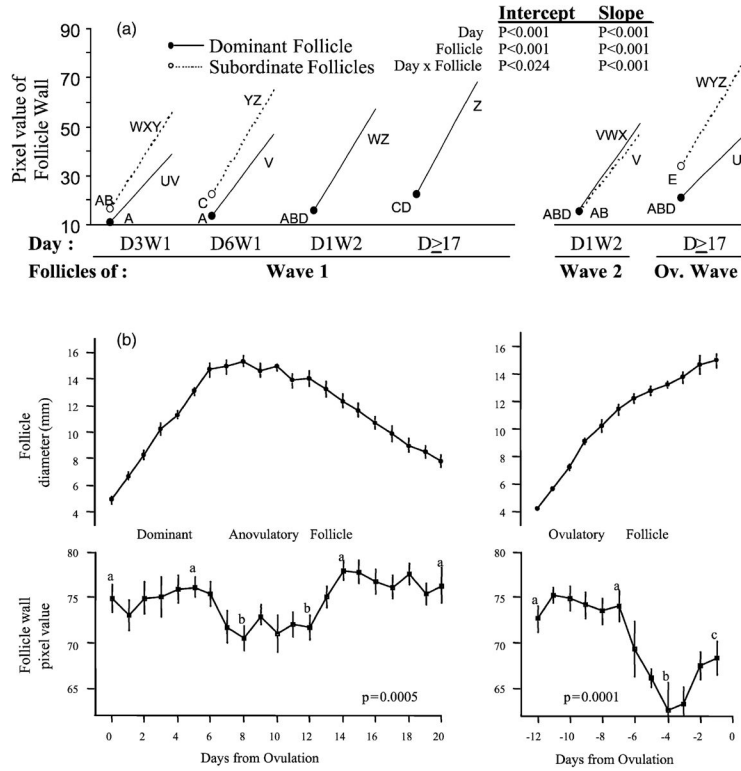
Fig. 8.
(a) Intercept (circles) and slope of regression lines obtained by line-analysis of the follicle wall of the dominant and subordinate bovine follicles. Values with no common letters indicate significantly different values ($P < 0.05$) in intercept (A, B, C, D, E) and slope (U, V, W, X, Y, Z) (modified from Singh et al., 1998). (b) Diameter profiles and associated echotexture characteristics of dominant anovulatory and ovulatory follicles in cattle (mean ± S.E.M.; $n = 15$ observations per day). The growing (days 0–6) and regressing phases (more than day 12) of the dominant anovulatory follicle are separated by a static phase (days 6–12). Values with no common superscripts indicate significant difference ($P = 0.05$) (modified from Tom et al., 1998).
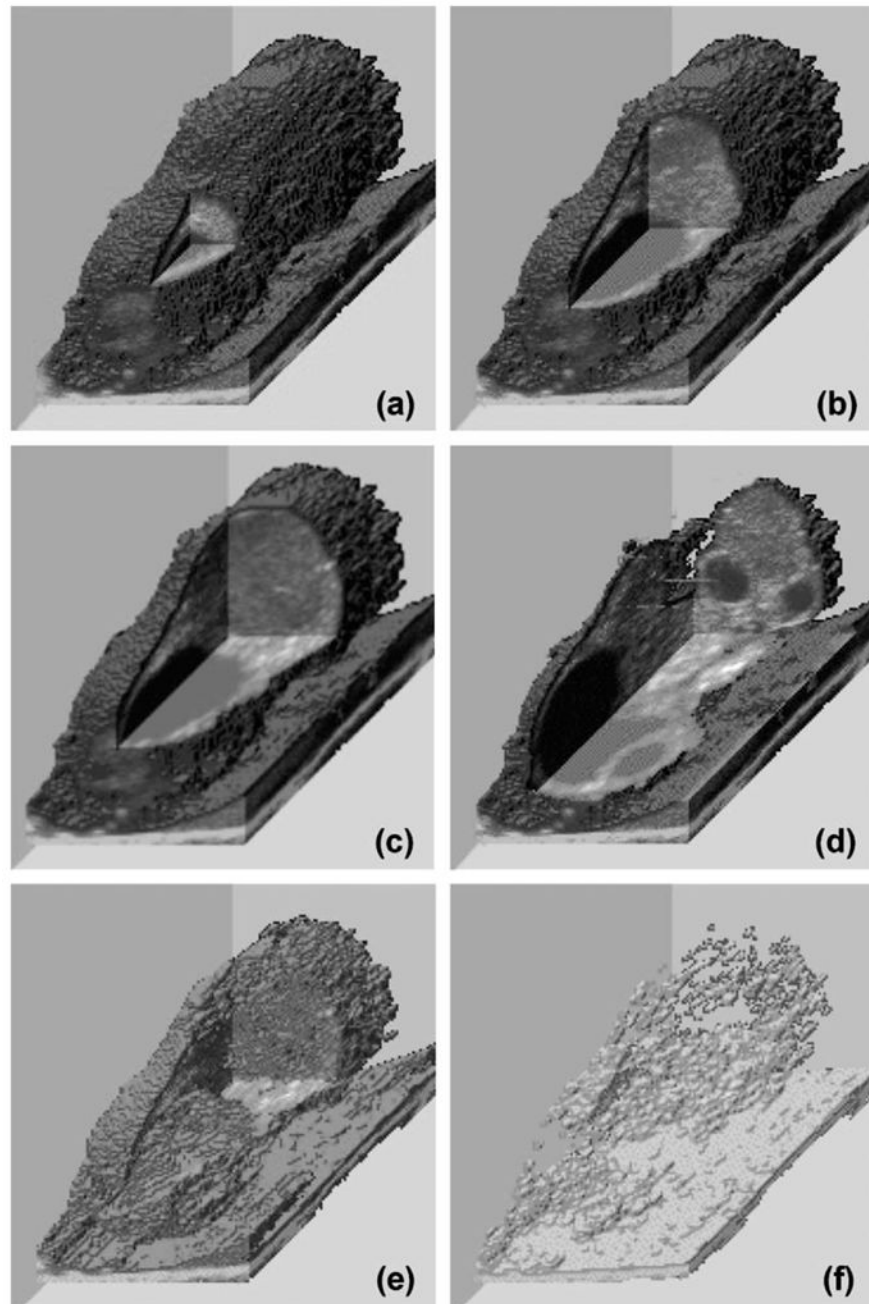
Fig. 9.
Reconstructed 3D ultrasonographic images of a bovine ovary with cutout portions (a–d) to expose the topographic locations of ovarian follicles and corpus luteum. Different transparency levels (d–f) allow the 'dissolution' of various structures.
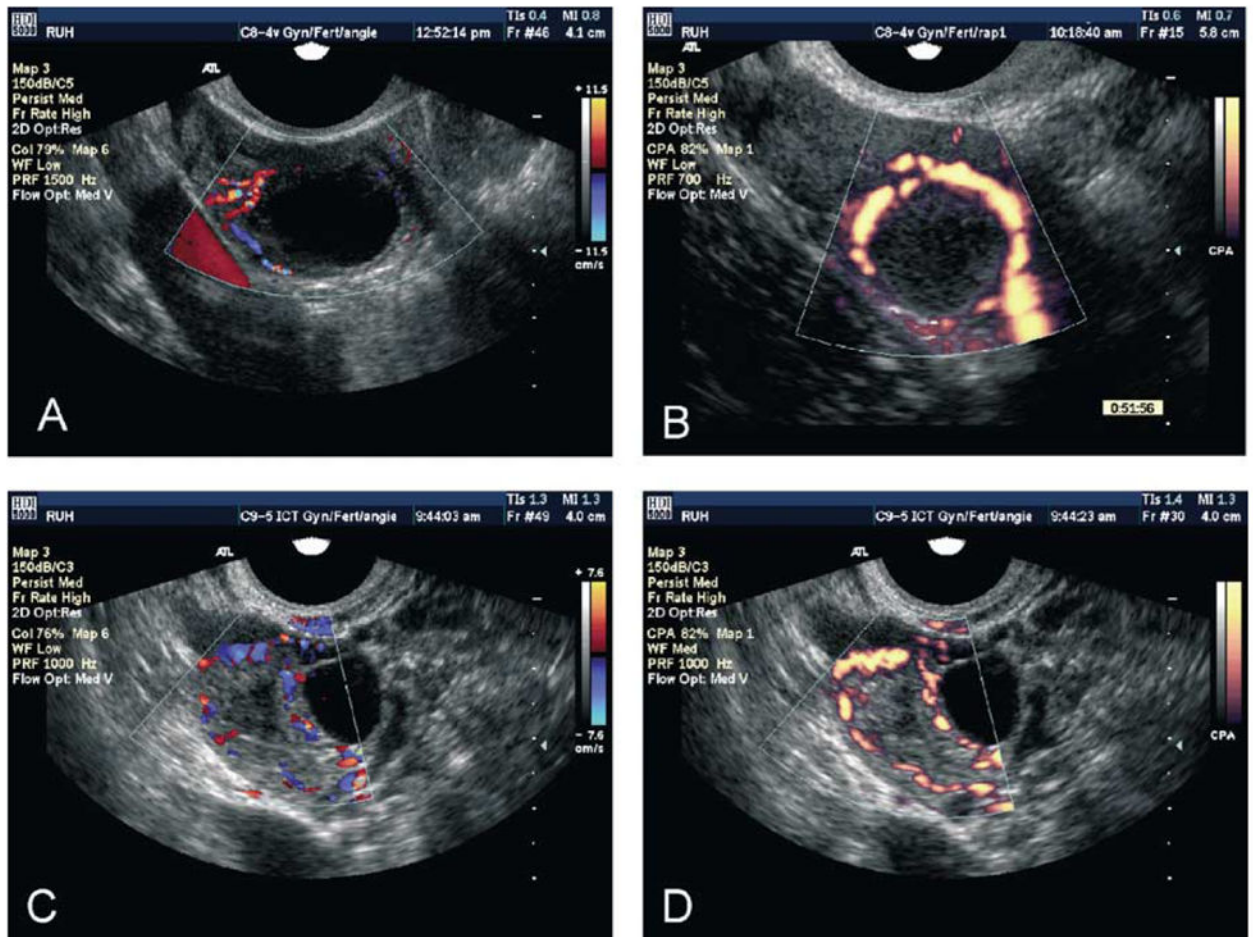
Fig. 10.
Color flow (A, C) and power flow Doppler ultrasound images of imminently preovulatory follicles (A, B) demonstrating directional peri-follicular flow and recent sites of ovulation (C, D) demonstrating the vascular patterns around walls of the recently collapsed follicle/ developing corpus luteum. In color flow images, blood flow toward the transducer is displayed in red, while flow away from the transducer is displayed in blue. In power flow images, all flow is displayed in a graded variant of yellow to orange colors.
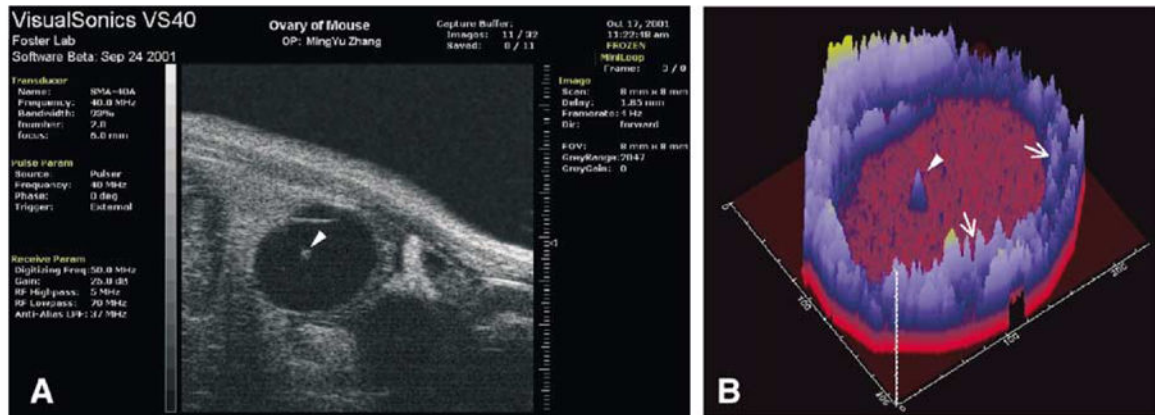
Fig. 11.
A. High resolution image of an ovarian follicle of an anesthetized mouse obtained by transabdominal scanning with the ultrasound biomicroscope. The resolution obtained is far greater than that obtained in Fig. 3A. Compared to the image of bovine follicle (Fig. 3A), the mouse follicle was much smaller (2.4 mm vs. 15 mm) and was imaged in situ (live) rather than in vitro (excised ovary in a water bath). The cumulus-oocyte-complex (arrowhead) is visible in the center of the follicle. (B) Region analysis of the ultrasound image in A was performed and never-before seen details of the follicle wall (arrows) and the cumulus–oocyte-complex (arrowhead) are clearly evident.
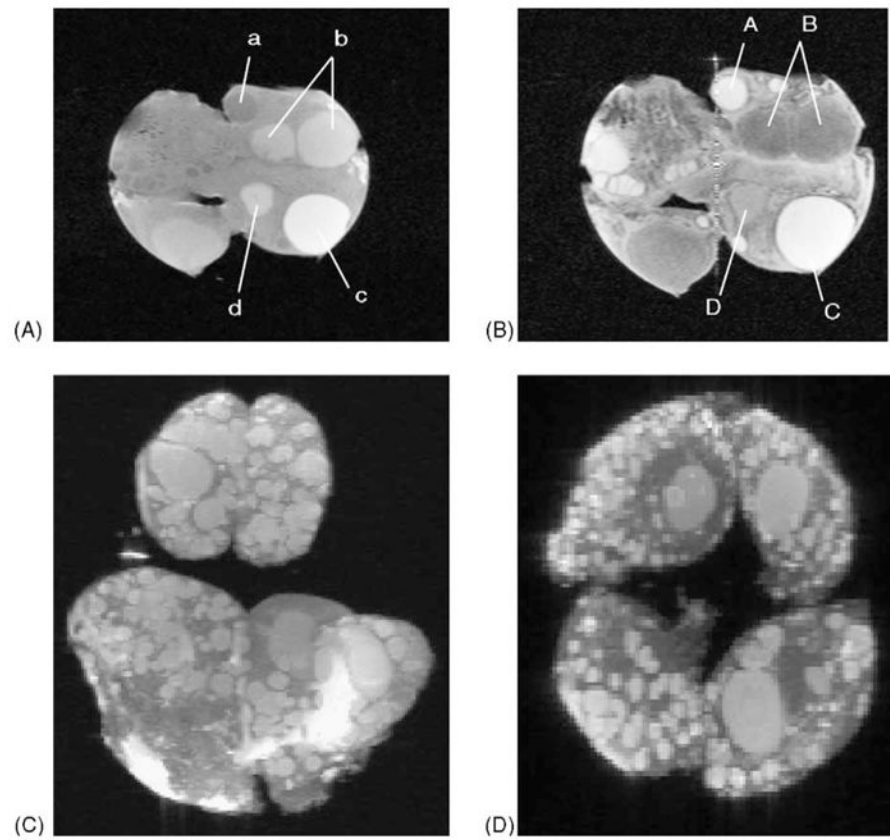
Fig. 12.
MRI images of an ex vivo bovine ovary in two A, B and three C, D dimensions. Two-dimensional T_1- (A) and T_2-weighted images demonstrating follicles in different stages of atresia (a, A, b, B), the physiologically dominant follicle (c, C) and a corpus albicans (d, D). Small follicle of 2 mm diameter were easily visualized. Three dimensional images created using FISP and PFISP imaging. Follicles and luteal structures are clearly identifiable in all views. The images may be rotated 360° in the computer. Adapted from Hilton et al., 2000 and Sarty et al., 2000.
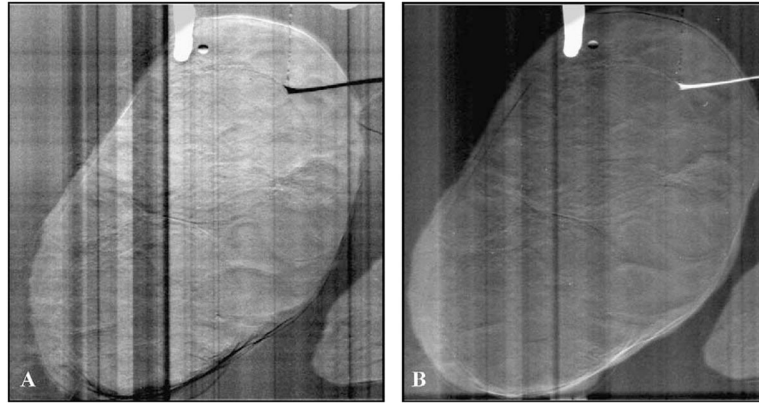
Fig. 13.
Diffraction enhanced images (DEI) of a bovine ovary produced with X-rays on beamline ×15A of the National Synchrotron Light Source, Brookhaven National Laboratory, Upton, NY. Three antral follicles approximately 4 mm in diameter are indicated on the left, and a corpus luteum is outlined on the right. The images were acquired on opposite sides of the diffraction rocking curve, resulting in opposing contrast. Artifact was produced by a paper clip (at top) used to suspend the ovary in a plexiglass water bath (vertical striations).